Appl. Phys. B 64, 301–305 (1997)

Applied Physics B Lasers and Optics

Intracavity frequency-doubled diode-pumped Nd : $LaSc_3(BO_3)_4$ lasers

V. G. Ostroumov[1], F. Heine[1], S. Kück[1], G. Huber[1], V. A. Mikhailov[2], I. A. Shcherbakov[2]

[1] Universität Hamburg, Institut für Laser-Physik, Jungiusstraße 9a, 20355 Hamburg, Germany
(Fax: + 49-40/4123-6281, E-mail: heine@physnet.uni-hamburg.de)
[2] General Physics Institute, Academy of Sciences of Russia, Vavilov Str. 38, 117942, Moscow, Russia

Received: 30 April 1996/Revised version: 1 July 1996

Abstract. An intracavity frequency-doubled 10%Nd : $LaSc_3(BO_3)_4$ (Nd : LSB) laser was investigated in different resonator configurations and in different operation modes under continuous wave (cw) and quasi-cw laser-diode pumping. With a Cr^{4+} : YAG passive modulator and a KTP crystal the second-harmonic output power at 531 nm amounted to 190 mW in *Q*-switched TEM_{00} mode at 750 mW of pump power. In a sandwich resonator, when all the optical elements were in direct contact with each other, 0.8 W of green output power was obtained in cw mode under 2.7 W of pump power with a slope efficiency of 44%. In the same setup under fiber-coupled diode-laser array pumping (5.6 W of incident power), 1.2 W of green output power was achieved in cw mode and 1.4 W in quasi-cw mode.

PACS: 42.60B; 42.65; 42.70

Compact, rugged and efficient diode-pumped solid-state lasers in the visible spectral region are required for many applications. High-efficiency intracavity frequency doubling with KTP and LBO crystals has been reported recently [1–6]. Conversion efficiencies exceeding 20% with respect to the pump power were obtained in Nd : YAG [1] and Nd : YVO_4 [2, 3] by internal frequency doubling with a KTP crystal and efficiencies of 10% and 30% for Nd : YLF and Nd : YVO_4 by using a LBO frequency doubler [5, 6]. Second-harmonic generation (SHG) of a miniature Nd : YVO_4 and Nd : $LaSc_3(BO_3)_4$ (Nd : LSB) laser with a KTP crystal in a simple resonator design is described in [7–9]. The main features of Nd : LSB crystals [10] are broad absorption bands (FWHM $\approx$ 3 nm) centered at 808 nm, large absorption coefficients (36 cm^{-1} for a typical 10% Nd^{3+} concentration that corresponds to an ion concentration of 5×10^{20} cm^{-3}), and very low losses at 1.06 µm ($< 10^{-4}$ cm^{-1}). Short nonlinear crystals of 0.5–2 mm in length were found to be adequate for efficient intracavity doubling and were less sensitive to misalignment and temperature changes, than a long crystal. Furthermore, the small nonlinear coupling decreases the "green problem". The SHG output power at 531 nm was more than 500 mW at 2 W incident power of a laser diode [8]. The practical needs demand further improvement of a microchip laser by decreasing dimensions and costs, increasing their efficiency at low pumping levels, improving stability and providing the possibility of operation in a *Q*-switched mode. The laser costs and dimensions can be decreased by using a sandwich-type resonator when all optical elements (directly coated gain media, intracavity frequency doubler and passive *Q*-switch modulator) are in direct contact to each other. This setup is easy to fabricate stable, and requires practically no adjustment. As compact and reliable *Q*-switch modulators for 1 µm lasers it is convenient to use saturable absorbers like Cr^{4+}-doped YAG (yttrium aluminum garnet) or YSGG (Yttrium Scandium Gallium Garnet) crystals. The small cavity length (0.5–2 mm), which can be provided in case of a sandwich resonator, leads to very short (< 1 ns) and high peak power (several kW) pulses in *Q*-switched miniature lasers [11–14], resulting in efficient nonlinear frequency conversion [11, 15]. The laser itself fits into a package which has approximately the size of a conventional diode-laser package.

In this work, Nd : LSB crystals together with a KTP frequency doubler were investigated for operation in different regimes. Our experiments included frequency doubling in continuous wave (cw) and *Q*-switch mode at low pump levels (< 800 mW), cw frequency doubling at moderate (up to 3 W) and at high pump power levels (up to 6 W) in cw and quasi-cw modes. We compared the sandwich resonator design with a normal plane–plane resonator at low and moderate pumping levels.

1 Laser experiments

Efficient intracavity frequency conversion can be achieved only at high-radiation densities, which can be provided by a low-loss resonator. The nonlinear dependence of the SHG output on pump power makes it especially difficult to obtain high conversion efficiencies at low pumping levels. Therefore, all resonator elements used in our experiments were preliminary selected for low passive losses. In order to maintain a high intracavity intensity, we used laser crystals that are able to deliver intracavity power densities of 1–10 MW/cm^2 at pump power levels of 700 mW in a HR–HR (Highly Reflective) resonator.

2 Q-switched laser

The typical experimental setup for diode pumping experiments is shown in Fig. 1a. We used a Siemens SFH-483401 1 W laser diode (emitting area: 200 μm × 1 μm) for low pumping levels and a LDP 4380C-5-C 3 W laser diode (emitting area: 380 μm × 1 μm) for moderate pumping levels. The divergent laser-diode beam was first collimated by a 5 mm focal length spherical lens. With this collimator, the plane of the beam perpendicular to the emitting surface is collimated, and the parallel component diverges. A cylindrical lens of 80 mm focal length behind the collimator was used to correct the astigmatism and therefore to collimate the diverging component, leaving the other plane unchanged. Finally, the beam was focused by a 30 mm focal length spherical lens onto the front surface of a crystal. The diode-pump focus at the $1/e^2$ intensity level was measured to be about 280 μm × 15 μm for the 1 W diode and 400 μm × 18 μm for the 3 W diode. The plane–plane resonator was formed by 1.06 μm HR (high-reflective) mirrors, directly coated on the front surface of 10%Nd:LSB crystals, which was also Anti-Reflective (AR) coated for 808 nm, and on the back surface of the KTP crystals. The inner face of the KTP was AR coated for 1.06 μm and 531 nm and that of the Nd:LSB was AR coated for 1.06 μm and HR for 531 nm. As passive *Q*-switch modulators we used Cr^{4+}:YAG crystals AR coated on both sides for 1.06 μm, with different initial transmissions at 1.06 μm (96–83%) and different lengths (0.5–2 mm). The total resonator length slightly exceeded the sum of the crystal lengths and was in the range of 3–7 mm. The laser crystals used in our experiments were 1 mm thick and were oriented to have maximum absorption ($\geq 90\%$) of the polarized pump radiation. The KTP crystals were 1 and 3 mm in length and selected for high optical quality.

The best input–output curve for the second-harmonic generation in a *Q*-switched mode is shown in Fig. 2. The average output power obtained with a 96% initial transmission Cr^{4+}:YAG modulator was 190 mW with a slope efficiency of 30%. Similar parameters were obtained for the modulators with initial transmissions down to 89%. This means that the efficiency of the laser is insensitive to the modulator transmission in a relatively wide range. The output power in cw mode, obtained in the same setup, but without the modulator, was slightly lower and is also given in Fig. 2 for comparison. The conversion efficiency of the incident pump power into the green output power was about 23 and 20% for *Q*-switch and cw modes, respectively. In comparison to the optimally coupled laser at 1.06 μm, we reached a conversion efficiency of 39 and 32% for 531 nm *Q*-switch and cw operation (Figs. 2 and 4).

The pulse duration and the repetition rate of the laser depend on the unsaturated transmission of the modulator and on the pumping rate (Fig. 3). By varying the initial transmission of the modulator and the pump power, it is possible to change the repetition rate in the range of 10–100 kHz and the pulse duration between 5 and 30 ns, keeping the laser efficiency high. The complex interactions of simultaneous intracavity frequency doubling and passive *Q*-switch in a microchip resonator are not completely understood. Formation of the short pulses by a saturable absorber will be opposed by the enhanced conversion of

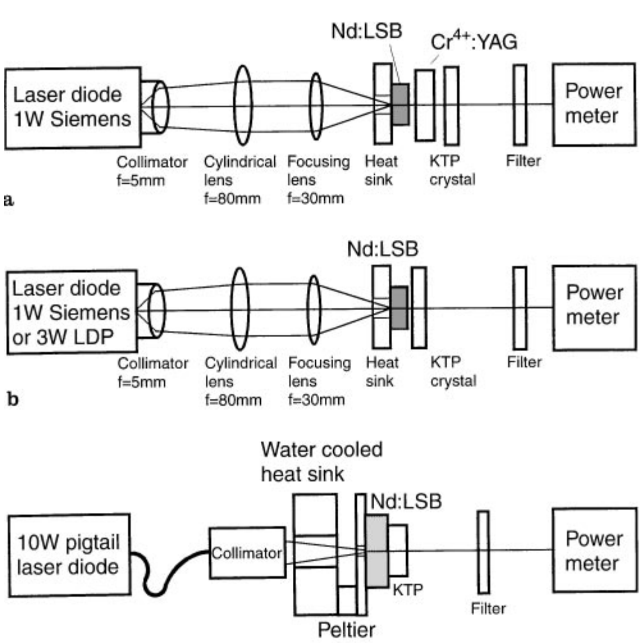

Fig. 1a–c. Experimental setup for the diode-laser pumping experiments: **a** for *Q*-switch experiments, **b** for cw experiments, **c** for high-power pumping with a fiber-coupled diode-laser array

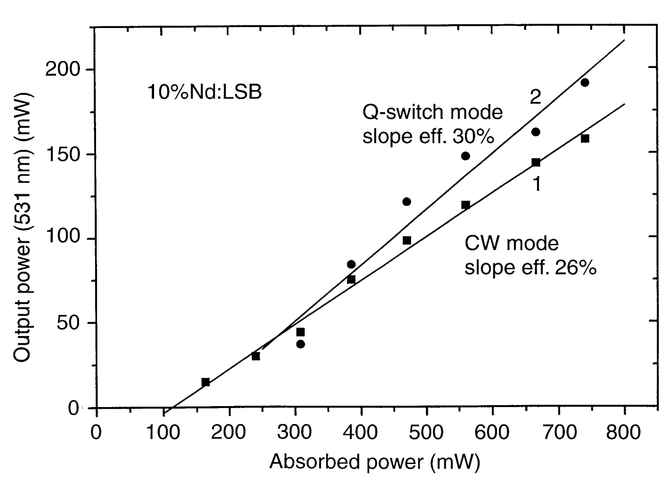

Fig. 2. Output power at 531 nm vs absorbed power for the 10% Nd:LSB in a 3 mm long resonator and 2 mm long KTP. *Trace 1*: cw mode, *trace 2*: *Q*-switch mode, (initial transmission of the Cr^{4+}:YAG: $T = 96\%$)

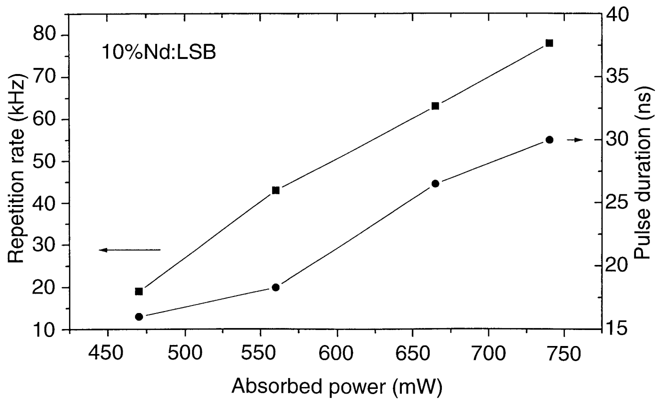

Fig. 3. Pump power dependence of SHG pulse duration and repetition rate for the 10%Nd : LSB. Resonator length is 3 mm, initial transmission of Cr^{4+} : YAG is $T = 96\%$

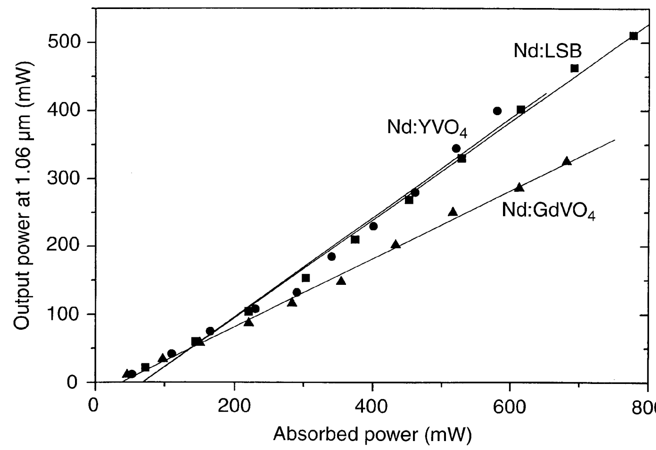

Fig. 4. Input vs output power at 1.06 µm for 10% Nd : LSB (*squares*), 1%Nd : YVO_4 (*circles*), and 1.1% Nd : $GdVO_4$ (*triangles*)

short pulses into the green. Numerical calculations are in progress.

The pulsed Nd : LSB laser was operating in a TEM_{00} mode at 531 nm in the whole range of pumping. This was the main difference compared to the cw regime: in this setup single transverse mode oscillation was possible only up to 80 mW of output power. The improved beam quality was due to the suppressing of high-order transversal modes by the Cr^{4+} : YAG modulator.

For comparison, we also investigated 1%Nd : $GdVO_4$ and 1%Nd : YVO_4 crystals under the same pumping conditions. The input–output dependence for all three crystals at 1.06 µm in cw mode are depicted in Fig. 4. Nd : LSB and YVO_4 crystals had nearly the same output and efficiency, while the slope efficiency of $GdVO_4$ was lower due to the higher crystal losses. In these experiments, we used a 5 cm radius of curvature output coupler with optimal transmissions which were 5% for the YVO_4 and $GdVO_4$ crystals and 1% for Nd : LSB. Frequency-doubling experiments in a plane–plane resonator setup, used earlier for Nd : LSB, revealed that for the vanadate crystals, the output power was 2–4 times lower than for Nd : LSB, both in cw and *Q*-switch mode. The difference, from our point of view, is mainly due to the significantly lower losses of Nd : LSB. Another reason for the higher performance of Nd : LSB is larger thermal lensing in this material. Thermal lensing in Nd : LSB seems to be optimal at these low levels of pumping: it is enough to stabilize the plane–plane resonator and to provide efficient lasing and, on the other hand, not too large to prevent single transversal mode oscillation. Vanadate crystals with comparable temperature dependence of refractive index dn/dT and similar absorption coefficients have thermal conductivity approximately 2 times higher than Nd : LSB and these crystals should be the material of choice for higher pump densities [6], where the aberration of the thermal lens is severe. This fact was also noted in [16], when the thermal focusing increased the mode size and increased the efficiency at higher pumping.

In other experiments we have set all the optical elements (Nd : LSB, modulator and KTP) into tight contact with each other (sandwich resonator). The setup provided lasing as efficient as for the short resonator, discussed above. The advantage of a sandwich laser is higher stability, due to the decreased vibration sensitivity of the optical elements, and simple alignment. Such resonators open realistic possibilities for monolithic low-threshold high-efficiency green lasers, especially with the use of advanced composite bond technologies [17].

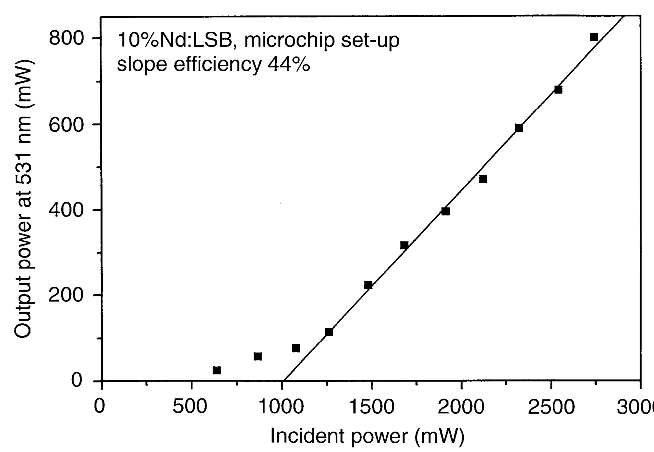

Fig. 5. Input vs output power for the Nd : LSB green laser with the 3 W diode laser pump

3 Cw 800 mW green laser

A KTP crystal, 1 mm long, was directly mounted on the surface of the Nd : LSB crystal (Fig. 1b). The crystal coatings were the same as in the *Q*-switch experiments. With a 3 W laser diode, we achieved 800 mW of output power at 531 nm with a slope efficiency of 44% and an overall efficiency of 30% with respect to the incident power (Fig. 5). The beam had an elliptical shape and was transversal multimode.

For Nd : LSB crystals, the temperature in the pump channel depends in first approximation linearly on the absorbed power with a constant of 70–90 K/W [18]. At 3 W pumping, the temperature in the pump channel is more than 200 K above the heat-sink temperature. This induces strong thermal lensing in the laser crystal (and also heats the KTP when both crystals are in direct contact). We observed in our experiments that cooling of LSB crystal did not increase the second-harmonic output in the whole pumping range. The reasons for this behavior are not clear yet.

4 High-power fiber-coupled diode pumping

In order to estimate the scalability of our cw system to higher pump powers, we performed diode pumping with a 10 W SDL-3450-P5 fiber-coupled laser-diode array (Fig. 1c). The fiber core diameter was 400 μm. We performed diode pumping with two different focusing systems and also without any optics between the laser and fiber (close coupling) in cw and pulsed modes. In the first experiment, the diode radiation was collimated and focused by a pair of 30 mm focal length spherical lenses AR coated for 808 nm. In another experiment, we used a commercially available T12 Schaefter & Kirchhoff collimator (S&K) with a numerical aperture NA = 0.54. For the latter case, the working distance between the end of the fiber and the entrance of the collimator is about 1.8 mm, resulting in a better coupling efficiency in comparison to the first case. Both collimators achieved a 1 : 1 image of the pump fiber aperture onto the crystal surface. The Nd : LSB and KTP sandwich resonator were mounted on a 0.5 mm thick copper plate with a 2 mm hole for the pump beam. The plate could be cooled by a Peltier cooler, mounted on the water-cooled heat sink (Fig. 1c).

With the S&K collimator, we achieved 1.2 W of cw output power at 531 nm with a slope efficiency of 30% (Fig. 6a). That was slightly better than for the combination of the pair of 30 mm focal length lenses. In both cases, the beam profile of the green output was a circular multitransversal mode. Above 3.8 W pump power, the Nd : LSB had to be cooled in order to maintain a high laser efficiency. The decrease in the slope efficiency in comparison to that under 3 W diode pumping was caused mainly by the larger pump focus and broader diode laser emission bandwidth, which decreased the pump power density. At pumping rates higher than 5.6 W, the output power of the green laser decreased dramatically and could not be restored by cooling the laser crystal. A high temperature in the pump channel significantly decreases the emission cross-section at 1.06 μm and creates strong temperature gradients, producing a very short focal length thermal-induced lens. Both factors reduce the overall laser efficiency due to an increasing lasing threshold and a decreasing overlap of the pump and laser mode size. The input–output curve is depicted in Fig. 6a. The beam-quality parameters M_y^2 and M_x^2 for vertical and horizontal directions were determined in the same way as it was done in [19]. The output beam at 531 nm appeared to have a Gaussian intensity profile, but the beam-quality parameter was far from unity, even for low pump levels (Fig. 7). This can be explained by the fact that the size of the TEM_{00} mode of the green laser is much smaller than the pump focus spot size and therefore many higher-order transversal modes oscillate.

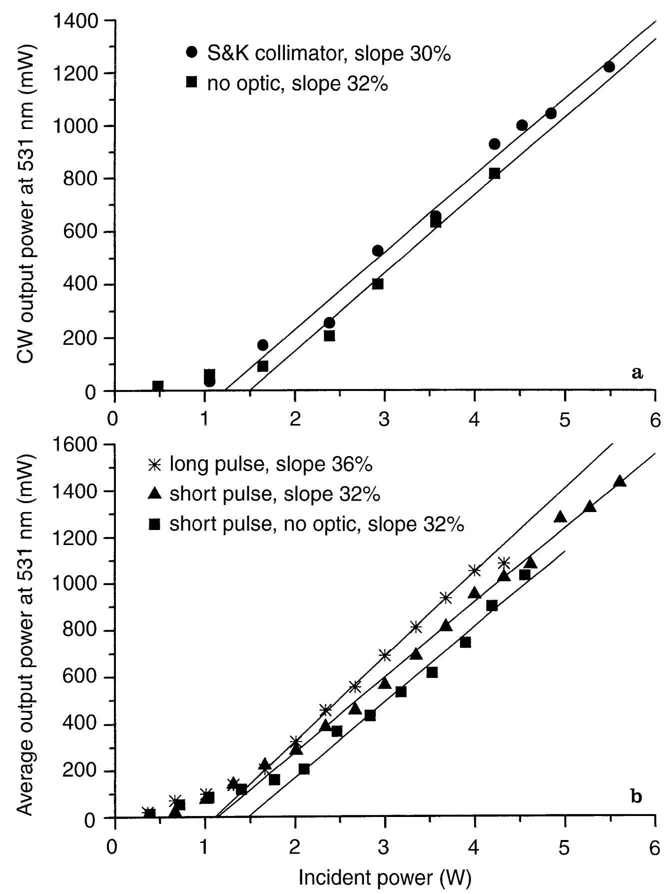

Fig. 6. Input vs output power for the microchip Nd : LSB laser at 531 nm, pumped by a 10 W fiber coupled diode array. *Circles* – S&K collimator, *squares* – no focusing optics between fiber end and the laser crystal **a** cw mode, *points* – S&K collimator, *squares* – close-coupled setup; **b** pulsed mode, *stars* – long pulse ($T_p = 0.05$ s), *triangles* – short pulse ($T_p = 0.005$ s) with S&K collimator, *squares* – short pulse mode in a close-coupled setup

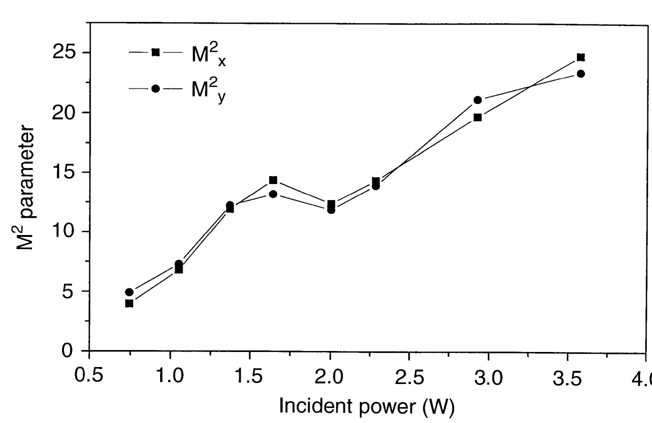

Fig. 7. Dependence of the M^2 beam parameter on the incident power of the 10 W fiber-coupled laser-diode array. *Squares* are for the *X* component and *circles* are for *Y* component

At an output power of about 600 mW at 531 nm, the stability and noise parameters were investigated. The output power of the microchip green laser had good long-term stability as well as a noise level of less than 2%

(peak-to-peak amplitude variation) in the 20 Hz–1 MHz frequency band. This is much better than the results obtained in setups where the gain and doubling crystals were separate. The reason for higher noise in these setups is an increased sensitivity against vibrations.

The microchip setup was also tested under quasi-cw pumping. We used two pumping modes: "long pulse" ($T_p = 0.05$ s) and "short pulse" ($T_p = 0.005$ s). Both modes had a 1 : 1 duty cycle. In the quasi-cw mode we were able to get 1.4 W of average output power at 531 nm with a slope efficiency of 32%.

Similar results were obtained without any focusing optic (close coupled setup) between the crystal and the fiber end.

The results for the setups described above are presented in Fig. 6.

5 Conclusions

We have demonstrated an efficient intracavity-doubled green Nd : LSB laser with all elements in contact with each other, resulting in good output stability against thermal and acoustical distortions. The sandwich resonator showed the same efficiency as the plane–plane resonator with separate optical elements and had superior mechanical stability. The thermal-induced lens in the LSB crystals makes the resonator stable and provides a good overlap of the laser mode and the pump focus. In a Q-switched mode at low pumping levels (below 800 mW), the maximum output power achieved at 531 nm was 190 mW (TEM_{00} mode). The diode to green conversion efficiency and the slope efficiency reached 23 and 30%, respectively. Pumped by a 3 W laser diode, the maximum cw output power of Nd : LSB was 800 mW (531 nm) at 2.7 W of incident power and the slope efficiency reached 44%. An intracavity frequency-doubled Nd : LSB laser, pumped by a fiber-coupled diode array, produced 1.2 W of cw output power and 1.4 W in quasi-cw mode at 531 nm, resulting in 22 and 26% conversion efficiency compared to the pump power. The compact and rugged sandwich resonator design with its inherent stability is well suited for simple, reliable green light sources at moderate pump power levels. Because of the poor thermal properties, Nd : LSB crystals provide a high-quality laser beam at cw output powers less than 100 mW at 531 nm in a microchip design.

Acknowledgements. This work has been performed in cooperation between the Institute of Laser Physics of the University of Hamburg and General Physics Institute of the Academy of Sciences of Russia, Moscow and was supported by the BMBF (German ministry of education and research).

References

1. M. Oka, S. Kubota: Jpn. J. Appl. Phys. **31**, 513 (1992)
2. Y. Kitaoka, S. Ohmori, K. Yamamoto, M. Kato, T. Sasaki: Appl. Phys. Lett. **63**, 299 (1993)
3. W. Weichmann, L.Y. Liy, S. Kubota: In OSA Proc. *on Advanced Solid State Lasers*, Vol. 24, ed. by B.H.T. Chai and S.A. Payne (Optical Soc. America, Washington, DC 1995) p. 96
4. P.S. Durkin, S.G. Post: In *OSA Proc. on Advanced Solid State Lasers*, Vol. 20, ed. by T.Y. Fan, B. Chai (Optical Soc. America, Washington, DC 1994) p. 332
5. G.A. Rines, R.A. Schwarz, P.F. Moulton: In *OSA Proc. on Advanced Solid State Lasers*, Vol. 20, ed. by T.Y. Fan, B. Chai (Optical Soc. America, Washington, DC 1994) p. 336
6. W.L. Nighan, Jr., J. Cole: *Advanced Solid State Lasers*, 1996 OSA Tech. Dig. (Optical Soc. America, Washington, DC 1996) postdeadline paper PD4
7. N. MacKinnon, B.D. Sinclair: Opt. Commun. **105**, 183 (1994)
8. J.-P. Meyn, G. Huber: Opt. Lett. **19**, 1436 (1994)
9. J.-P. Meyn, G. Huber: In *Conf. on Lasers and Electro-Optics*, 1995, OSA Tech. Dig. Ser., Vol. 15 (Optical Soc. America, Washington DC, 1995) p. 78
10. J.P. Meyn, T. Jensen, G. Huber: IEEE J. **QE-30**, 913 (1994)
11. J.J. Zayhowski, C. Dill III: Opt. Lett. **17**, 1201 (1992)
J.J. Zayhowski, C. Dill III: Opt. Lett. **19**, 1427 (1994)
12. S. Zhou, K.K. Lee, Y.C. Chen, S. Li: Opt. Lett. **18**, 511 (1993)
S. Zhou, K.K. Lee, Y.C. Chen, S. Li: Opt. Lett. **18**, 1418 (1993)
13. L. Fulbert, J. Marty, B. Ferrand, E. Molva: In *Conf. on Lasers and Electro-Optics*, 1995, OSA Tech. Dig. Ser. Vol. 15 (Optical Soc. America, Washington, DC 1995) p. 176
14. B. Braun, F.X. Kärtner, U. Keller, J.-P. Meyn, G. Huber: Opt. Lett. **21**, 405 (1996)
15. J.J. Zayhowski, J. Ochoa, C. Dill III: In *Conf. on Lasers and Electro-Optics*, 1995 OSA Tech. Dig. Ser., Vol. 15 (Optical Soc. of America, Washington, DC 1995) p. 139
16. W.L. Nighan, Jr., D. Dudley, M.S. Keirstead: In *Conf. on Lasers and Electro-Optics*, 1995, OSA Tech. Dig. Ser., Vol. 15 (Optical Soc. of America, Washington, DC 1995) p. 17
17. Onyx Optics, Application Note, June 1995, Onyx Optics Pleasanton, CA 94588
18. V.G. Ostroumov, T. Jensen, J.-P. Meyn, G. Huber, V.B. Tsvetkov, I.A. Shcherbakov: In *Conf. on Lasers and Electro-Optics*, Europe Tech. Dig. (1994) p. 59
19. B. Neuenschwander, R. Weber, H.P. Weber: IEEE J. **QE-31**, 1082 (1995)